On the importance of many-body interactions in the effective fluid model of asymmetric hard-sphere mixtures

2003 J. Phys.: Condens. Matter 15 S3443

(http://iopscience.iop.org/0953-8984/15/48/005)

INSTITUTE OF PHYSICS PUBLISHING JOURNAL OF PHYSICS: CONDENSED MATTER

J. Phys.: Condens. Matter **15** (2003) S3443–S3453 PII: S0953-8984(03)66403-9

On the importance of many-body interactions in the effective fluid model of asymmetric hard-sphere mixtures

S Amokrane[1], **A Ayadim and J G Malherbe**

Groupe de Physique des Milieux Denses, Faculté des Sciences et de Technologie, Université Paris XII, 61 Avenue du Général de Gaulle, 94010 Créteil Cedex, France

E-mail: amokrane@univ-paris12.fr

Received 18 July 2003
Published 20 November 2003
Online at stacks.iop.org/JPhysCM/15/S3443

Abstract

Comparison of solute pair distribution functions in the true mixture and in the effective fluid is used as a diagnosis of the importance of many-body interactions in the effective fluid model of binary asymmetric hard-sphere mixtures. Results from integral equations and density functional theories are compared with simulation data for size ratios $R = 3.33$, 10 and 20. Small deviation from the pair interaction approximation are detected up to $R = 20$. The origin of these deviations suggests that many-body effects might be more important in non-hard-sphere mixtures exhibiting long range solute–solvent correlations.

1. Introduction

The theoretical description of colloidal suspensions at the effective fluid level considers a one-component system of solute particles interacting via a coarse-grained potential obtained by integrating out the degrees of freedom of the other components of the mixture. From a practical point of view, one is often forced to adopt such a one-component description because the direct treatment of 'true' mixtures meets particular difficulties, both in the 'analytical' routes and in the simulation one, which is necessary at least to validate the unavoidable approximations made using the former route. This formal mapping onto an effective one-component fluid is exact as long as one retains the many-body nature of the coarse-grained interaction, whose exact evaluation is, however, impossible. In practice, this procedure is thus used only under the pair additivity assumption, which ignores contributions beyond two-body interactions (this will be referred to as the pair interaction approximation (PIA)). Since there is growing evidence that many-body interactions might be important even for uncharged colloids [1–3], it is important to assess the domain of validity of this assumption (see also [4] for a discussion of this point).

[1] Author to whom any correspondence should be addressed.

0953-8984/03/483443+11$30.00

The direct estimation of many-body effects at the theoretical level is actually difficult. One practical diagnosis of their importance is the comparison of structural quantities computed for the 'true' mixture and for the one-component fluid with effective pair interactions [2].

The simplest model for which such a programme can be carried out is the binary mixture of hard spheres (HS) with high diameter ratio $R = d_2/d_1 \gg 1$ (hereafter 1 and 2 refer to solvent and solute particles, respectively). This model has been widely studied in recent years to understand the phase behaviour of sterically stabilized colloids, essentially pseudo-binary colloid–colloid or colloid–polymer mixtures. The true HS mixture model is characterized by the size ratio R and the packing fractions η_1 and η_2 ($\eta_i = \frac{\pi}{6}\rho_i d_i^3$, with ρ_i the number density of component i). In the corresponding effective fluid with pair interactions, the total potential energy of the N_2 solute particles is $\phi(R^{N_2}; \mu_1) = \sum_{i<j} \phi^{\mathrm{HS}}(R_{ij}) + \phi^{\mathrm{eff}}(R_{ij}; \mu_1)$, where ϕ^{HS} is the direct HS interaction and ϕ^{eff} is the potential of the mean force at infinite dilution, in the pure solvent at chemical potential μ_1. If the correspondence between the thermodynamic variables (η_1, η_2) and (μ_1, η_2) is properly established, the PIA is the main source of possible differences between the solute pair distribution functions (pdf) in the true mixture and in the effective fluid, g_{22}^{mix} and g_{22}^{eff}, respectively. Calculations with the reference hyper-netted chain (RHNC) integral equation and density functional theories (DFT) complement a previous report [2] of a similar comparison from simulation. It is indeed important to check whether 'analytical' methods can provide reliable results, because simulations are particularly difficult when R exceeds unity by a large amount.

This work is presented as follows: after presenting in section 2 the theoretical methods used to compare g_{22}^{mix} and g_{22}^{eff}, results will be presented in section 3 for $R = 3.33$, 10 and 20 in order to estimate the domain of size ratio and packing fractions for which the pair approximation might be sufficient. The test by simulation of the non-additivity of the mean force will also be reconsidered briefly and the paper will end with a brief conclusion.

2. Theoretical methods

2.1. Formal mapping onto the effective fluid

The formal reduction of a (binary) mixture onto an effective one-component fluid is now well documented (see, for example, [5]). The convenient thermodynamic ensemble is the semi-grand one. The mixture with a fixed number of solute particles N_2 is in equilibrium with a reservoir of solvent particles with temperature T and chemical potential μ_1. The associated thermodynamic potential $F(N_2, V, T; \mu_1)$ is

$$F = -kT \ln Z(N_2, V, T; \mu_1) \tag{1}$$

with

$$Z = \frac{1}{N_2! \Lambda_2^{3N_2}} \sum_{N_1} \frac{z_1^{N_1}}{N_1!} \int_V \int_V \mathrm{d}\mathbf{r}^{N_1}\, \mathrm{d}\mathbf{r}'^{N_2} \exp[-\beta H(\mathbf{r}^{N_1}, \mathbf{r}'^{N_2})] \tag{2}$$

where $\beta = 1/kT$, $z_1 = \Lambda_1^{-3}\exp(\beta\mu_1)$ is the solvent fugacity with $\Lambda_i = h/\sqrt{2\pi m_i kT}$ and V is the volume of the mixture. Equivalently, Z can be written as

$$Z = \frac{1}{N_2! \Lambda_2^{3N_2}} \int_V \mathrm{d}\mathbf{r}^{N_2} \exp[-\beta(H_{22}(\mathbf{r}^{N_2}) + \Omega)] \tag{3}$$

with

$$\Omega = -kT \ln \sum_{N_1} \frac{z_1^{N_1}}{N_1!} \int_V \mathrm{d}\mathbf{r}'^{N_1} \exp(-\beta H_{11}(\mathbf{r}'^{N_1}) + H_{12}(\mathbf{r}'^{N_1}, \mathbf{r}^{N_2})) \tag{4}$$

where H_{ij} is the sum of the pair interaction terms u_{ij} between species i and j. Equations (2) and (3) are exact. They constitute the starting point of the effective one-component representation, Z appearing as the canonical partition function of a one-component system with thermodynamic variables (N_2, T, V) interacting through the effective N_2-body interaction potential $H^{\text{eff}} = H_{22} + \Omega$. In this treatment, the effect of the solvent on the solute particles is entirely contained in the indirect potential Ω. The latter depends on μ_1 and is a functional of the interaction potentials u_{11} and u_{12} through equation (4). Although the latter shows that there is little chance that Ω would be a sum of pair terms, its expression is, however, so intractable that direct estimation of the domain of validity of the PIA is impossible. In this approximation, one writes down Ω as an expansion in n-body terms:

$$\Omega = \Omega_0(\mu_1, T, V) + N_2\omega_1(\mu_1, T, V) + \sum_{i<j} \omega_2(\mathbf{r}_{ij}; \mu_1, T) + \text{higher-order terms.} \tag{5}$$

The analysis of the different terms in equation (5) is detailed, for example, in [5]. We just mention here that Ω_0 is the grand potential of the pure solvent at μ_1 and T. The one-body term $N_2\omega_1$ is the grand potential difference obtained by considering as independent the contribution of each solute particle in the solvent sea. The only relevant term for the phase behaviour of the effective fluid (at fixed μ_1 and T) is that involving ω_2 (a formal comparison of the free energies in the mixture and in the effective fluid is detailed in [6]). If the potential of the mean force is defined so that it vanishes when the N_2 solutes are all far apart, we are left with an effective fluid with pairwise additive interactions:

$$H^{\text{eff}} = \sum_{i<j}^{N_2} u^{\text{eff}}(r_{ij}; \mu_1, T) \tag{6}$$

with

$$u^{\text{eff}}(r; \mu_1, T) = u_{22}(r) + \omega_2(r; \mu_1, T) \tag{7}$$

where u^{eff} contains the direct part u_{22} of the solute–solute interaction and the indirect one ω_2 is mediated by the solvent. For a pure HS mixture, ω_2 reduces to the depletion potential (hereafter denoted ϕ^{eff}). For a given size ratio, ϕ^{eff} depends only on r and μ_1 (or ρ_1^{b}, the solvent density in the reservoir).

To complete the mapping, we need to establish the correspondence between the variables (η_1, η_2) and (μ_1, η_2) or equivalently $(\eta_1^{\text{b}}, \eta_2)$, where η_1^{b} is the solvent packing fraction in the reservoir. This is achieved in principle by solving the osmotic equilibrium equation:

$$\mu_1(\eta_1^{\text{b}}) = \mu_1(\eta_1, \eta_2). \tag{8}$$

Whereas the lhs of equation (8) can be evaluated from accurate equations of state for the one-component HS fluid, the rhs requires computing the solvent chemical potential in the mixture, which is a non-trivial task. Fortunately, several approximations have been tested against simulations [5]. The relation $\eta_1^{\text{b}}(\eta_1, \eta_2)$ was thus taken either from the scaled particle theory (SPT) expression or from that proposed in [7], which was recently found to work quite well.

2.2. g_{22}^{mix} and g_{22}^{eff} from DFT and RHNC

The pdfs were computed from Rosenfeld's fundamental measure functional (FMF) either in a pure DFT scheme, or from the RHNC closure of the Ornstein–Zernike equation (OZE), the bridge functions b_{ij} being obtained from the FMF [8]. Since both routes share the latter DFT, we begin by briefly recalling the main steps of a pure DFT calculation of the pdfs

(for a review of the DFT, see [9]). The starting point is the equation giving the density profile $\rho_i(r) = \rho_i(1 + h_i(r))$ for particles of type i, subject to an external potential $u_i(r)$:

$$\rho_i(r) = \rho_i \exp\{-\beta u_i(r) + c_i^{(1)}(r) - c_{i,o}^{(1)}(r)\}. \tag{9}$$

Equation (9) follows from the minimization of the grand potential $\Omega[\{\rho_i(r)\}]$. The latter is obtained from an assumed form of the excess free energy functional $\beta F_{\rm ex}^{\rm HS}[\{\rho_i(r)\}] = \int \mathrm{d}\mathbf{x}\, \Phi[\{n_\alpha(\mathbf{x})\}]$, where $\{n_\alpha(\mathbf{x})\}$ is a set of weighted densities constructed from the actual densities $\{\rho_i(r)\}$. ρ_i is the density of particles of type i far from the inhomogeneity. The one-particle direct correlation functions (dcf) given by the first functional derivative $c_i^{(1)}(r_1) = -\beta\delta F_{\rm ex}[\{\rho_i(r)\}]/\delta\rho_i(r_1)$ is minus the excess (with respect to the ideal gas) chemical potential functional in units of $k_{\rm B}T$: $c_i^{(1)}(r) = -\beta\mu_{i,\rm ex}[\{\rho_i(r);\}r]$. One thus has

$$\beta\mu_{i,\rm ex}^{\rm HS}[\{\rho_i(r)\}] = \sum_\alpha \frac{\partial\Phi[\{n_\alpha(r)\}]}{\partial n_\alpha} \otimes \omega_i^{(\alpha)}. \tag{10}$$

When equation (9) is used in the test particle limit ($u_i(r) = u_{ij}(r)$, the potential felt by a particle of type i created by the test particle j at the origin) the pdf i–j is

$$g_{ij}^{\rm DP}(r) = \exp\{-\beta u_{ij}(r) + (\mu_{i,\rm ex}[\rho_i(r); r] - \mu_{i,\rm ex}(\rho_i)\}. \tag{11}$$

For a homogeneous system, Rosenfeld's original FMF features the Percus–Yevick (PY) free energy density $\Phi(\{n_\alpha\})$. The dcfs obtained from successive functional derivatives of $F_{\rm ex}^{\rm HS}$ are also the PY ones. As recently shown by Roth *et al* [10] and Yu and Wu [11], to which one may refer for details, improved results are obtained by inputting the BMCSL [12] expression for Φ. This is the method used in this work.

At this stage, it is recalled that the pure DFT route does not involve the OZE, which relates the dcf and the pdf:

$$h_{ij} = c_{ij} + \sum_k \rho_k c_{ik} \otimes h_{kj} \tag{12}$$

where $h_{ij} = g_{ij} - 1$ is the total correlation function and $\otimes$ designates a convolution product. This must be supplemented by a closure relation

$$g_{ij}^{\rm OZ} = \exp\{-\beta u_{ij} + h_{ij} - c_{ij} - b_{ij}\} \tag{13}$$

with some approximation for the bridge function b_{ij}. The RHNC/FMF follows by recasting the density profile equation (9) in the form of a closure of the OZE (equation (13)). One thus gets [8]:

$$b_{ti}[\{\rho_i(r); r\}] = \beta(\mu_{i,\rm ex}^{\rm HS}[\{\rho_i g_{ti}(r); r\}] - \mu_{i,\rm ex}^{\rm HS}(\{\rho_i\})) + \tilde{\gamma}_{ti}(r) \tag{14}$$

where g_{ti} is the pdf for particles i in the field of the test particle and

$$\tilde{\gamma}_{ti}(r) = \sum_j \rho_j c_{ij}^{(2),\rm HS} \otimes h_{tj} \tag{15}$$

where $c_{ij}^{(2),\rm HS}$ is the two-body dcf obtained as the second functional derivative of $F_{\rm ex}^{\rm HS}$. It must, of course, also be computed [10, 11] from $\Phi^{\rm BMCSL}$.

We thus have two methods for computing the pdf: a pure DFT one ($g_{ij}^{\rm DP}$) and one from the OZ equation ($g_{ij}^{\rm OZ}$). While the latter should, in principle, be preferred for computing structural quantities (it obeys the OZE, which is a strong constraint), its major drawback is the existence of a domain in the (η_1, η_2) plane where the integral equation has no solution. In this case, we have to resort to the first method which usually does not exhibit this limitation to the same extent.

We finally stress here a problem that is common to both methods. Since the FMF is not an exact functional, the application of this formalism in the test particle limit does not guarantee

the symmetry requirement $g_{ij} = g_{ji}$ even when the species i and j play a symmetrical role in $F_{\rm ex}^{\rm HS}$. For preserving the symmetry in the indexes one introduces symmetrized bridge functions. Rosenfeld's ansatz is [13]

$$\bar{b}_{ti} = (x_i b_{ti} + x_t b_{it})/(x_i + x_t) \tag{16}$$

with x_i the concentration of component i. It is stressed here that b_{ti} is obtained from the bridge functional $B_i[\{\rho_m g_{tm}(r); r\}]$ relative to component i (it is a functional of all the pdfs g_{tm} in the field of the test particle t). Equation (16) is, however, not the only way to achieve symmetrization. The alternative

$$\bar{b}_{ti} = (x_i b_{it} + x_t b_{ti})/(x_i + x_t), \tag{17}$$

for example, does the same. Both were thus used in this work. (A more detailed discussion of this point will be given elsewhere. See also the recent work of Archer and Evans [14] for a discussion of this point.)

The next step is to obtain the effective potential. This is obtained by writing the previous equations at infinite dilution of the large spheres:

$$g_{22}(r; \rho_2 \to 0, \mu_1) = \exp[-\beta(u_{22}(r) + \Phi^{\rm eff}(r; \mu_1)]. \tag{18}$$

Here g_{22} is either $g_{ij}^{\rm OZ}$, as detailed for example in [15], or $g_{ij}^{\rm DP}$, in which case we recover the DFT calculation of Roth *et al* [16] (see [14] for a proof of the equivalence of the two routes).

Once $\Phi^{\rm eff}$ is known, $g_{22}^{\rm eff}$ is computed from the formalism outlined above in the one-component version. The situation is, however, not the same in the DFT and OZE routes. The former can be used only in the context of a mean field or similar approximate treatments, since we do not have functionals for arbitrary potentials. In this respect, the RHNC route assumes only universality [8] of the bridge *functional*—that is a much weaker assumption. Since the RHNC has been shown to work very well for 'depletion-like' potentials [15, 17], it will provide an essentially exact result for a given $\Phi^{\rm eff}$, say that obtained from the DFT route. This is the method we used to compare $g_{22}^{\rm mix}$ and $g_{22}^{\rm eff}$ when the RHNC for the mixture falls in the non-convergence domain.

2.3. g_{22}^{mix} and g_{22}^{eff} from simulation

The simulation data for $g_{22}^{\rm mix}$ and $g_{22}^{\rm eff}$ are essentially those presented in our previous work [2], except for $R = 20$, in the effective fluid. Other simulation data from the literature (obtained by Lue and Woodcock [18] and Malijewsky *et al* [19]) will also be compared with the analytical route. We just recall here that for the mixture our data were obtained with the cluster algorithm of Krauth *et al* [20] in the (N_1, N_2, V, T) ensemble.

To obtain $g_{22}^{\rm eff}$ the relation $\eta_1^{\rm b}(\eta_1, \eta_2)$ was taken from the SPT which has been tested versus simulation in [5]. At higher η_2, the more accurate expression given in [7] was used instead. The effective potential $\Phi^{\rm eff}(r; \eta_1^{\rm b})$ is first computed by a very long PCA run with two solute particles, as detailed in [2]. Once it is known, $g_{22}^{\rm eff}(r; \eta_1^{\rm b}, \eta_2)$ is computed in a second step by a standard (N_2, V, T) MC run.

3. Results and discussion

3.1. Effective potential

The determination of the effective potential is a preliminary step in the study of the effective fluid. We thus consider briefly here its determination from the methods outlined above. Calculation of the depletion potential by Roth *et al* [16] and those already presented in our

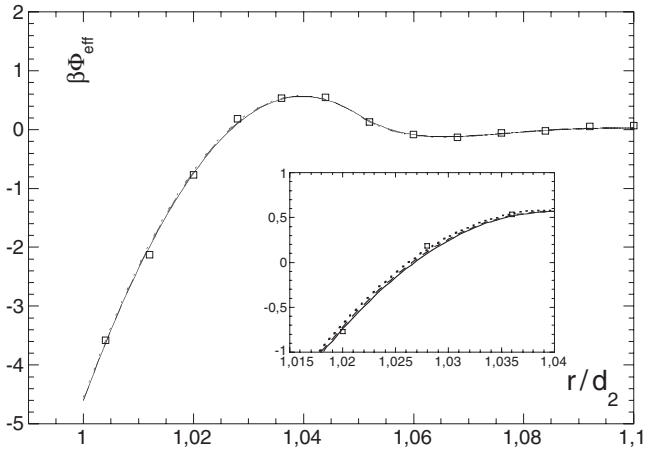

Figure 1. Depletion potential for $R = 20$ as a function of the reduced distance between solute particles, with a solvent bulk packing fraction $\eta_1^b = 0.14$. The inset shows an enlarged section to distinguish the three curves. Squares: simulation. Full curve: DFT (test part 1). Broken curve: RHNC (sym 1). Dotted curve: RHNC (sym 2).

previous work [2] has shown that the DFT and integral equation routes are now accurate enough, at least for the range of parameters R and η_1^b for which simulation data are available. An example is shown in figure 1 for $R = 20$. We indeed find an excellent agreement with simulation. Three different calculations are actually compared with simulation ($t1$ stands for a small test particle and sym 1 and sym 2 to equations (16) and (17), respectively). The bulk solvent packing fraction in the example shown is, however, not large enough to draw a definitive conclusion. We plan a more systematic comparison in the future in order to check whether the analytical route might eventually spare the simulation in the determination of the effective potential.

3.2. Pair distribution functions

g_{22}^{mix} and g_{22}^{eff} were compared for size ratios $R = 3.33$, 10 and 20. This regime corresponds rather to pseudo-binary colloid–colloid mixtures (though $R = 20$ is roughly the lowest limit for micro-emulsions in a molecular solvent).

To begin with, we first discuss the case $R = 10$. In our previous work, the coordination number $G(r) = \int_0^r \rho_2 g_{22}(r) 4\pi r^2 \, \mathrm{d}r$ was used as the criterion because simulation data for the pdfs are usually noisy. It was observed that, for fixed η_1^b, the effective fluid overestimates the coordination number but its variation with η_2 is moderate (when η_2 falls in the range accessible by the simulation algorithm). This overestimation seemed to increase with η_1^b according to the data we collected [2] (see also figure 5). Since in some instances we could obtain rather smooth pdfs, we compare here the simulation and the RHNC results in figure 2 for $R = 10$ and a low value of η_2. Besides the excellent agreement between simulation and RHNC, we observe here directly on the pdf the trend shown by the coordination number. Note that the overestimation is rather moderate since the relative change of the coordination number at $r = d_1 + d_2$ is about $\Delta G/G(r = d_1 + d_2) \simeq 6\%$ ($\Delta G/G = (G^{\mathrm{eff}} - G^{\mathrm{mix}})/G^{\mathrm{mix}}$). In order to check the argument [2] according to which the error due to the pair additivity assumption should not increase in relative magnitude with η_2, we show in figure 3 the results at a much higher value: $\eta_2 = 0.5$. The simulation data are from the work of Lue and Woodcock and the analytical

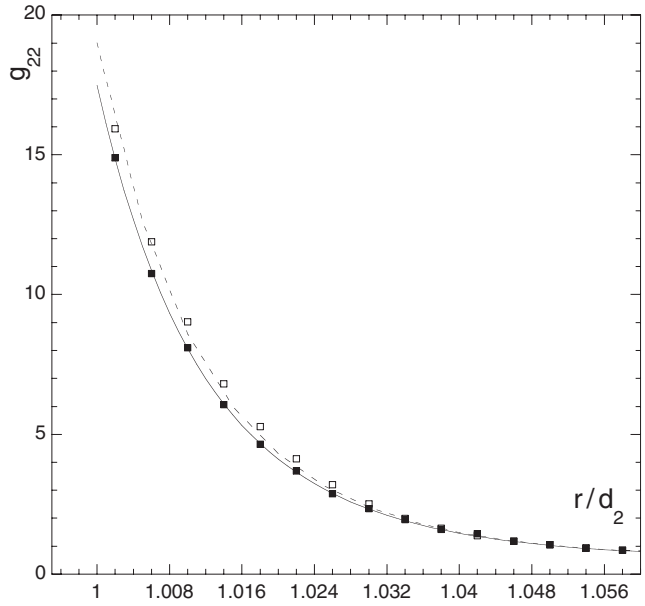

Figure 2. Solute pdfs for $R = 10$, $\eta_1^{\mathrm{b}} = 0.17$, $\eta_1 = 0.15$, $\eta_2 = 0.091$. Full curve: g_{22}^{mix}, broken curve: g_{22}^{eff}. Symbols: simulation; full squares: g_{22}^{mix}, empty squares: g_{22}^{eff}.

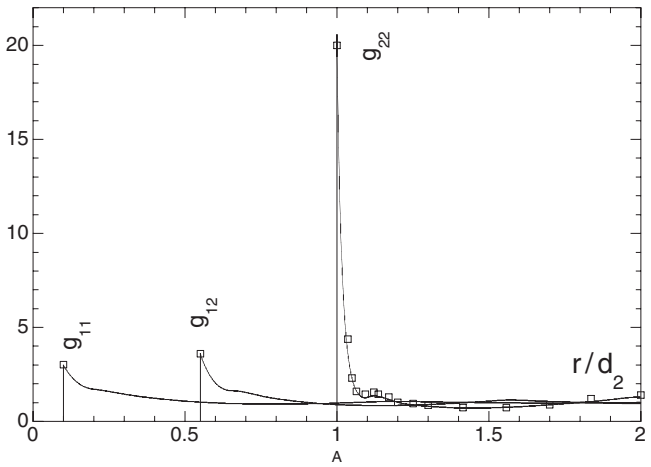

Figure 3. PDFs in a mixture with $R = 10$, $\eta_1 = 0.05$, $\eta_2 = 0.5$. Symbols: simulation from [18], curves: DFT.

results are pure DFT ones (except for the effective fluid), since the RHNC is in the no-solution domain. Note that we used a symmetrized version, i.e. we enforce $g_{12} = g_{21}$ through the equivalent of equation (16) for the chemical potentials in equation (9). Figure 3 shows the agreement of three pdfs with simulation (a similar comparison is made in [11]). In figure 4, which shows the comparison with the effective fluid, we again observe the overestimation in the contact region of g_{22}^{eff} as compared to g_{22}^{mix}. Note, however, that even with this high solute packing fraction, the effect is again small. We have, for example, $\Delta G/G(r = d_1 + d_2) \simeq 4\%$.

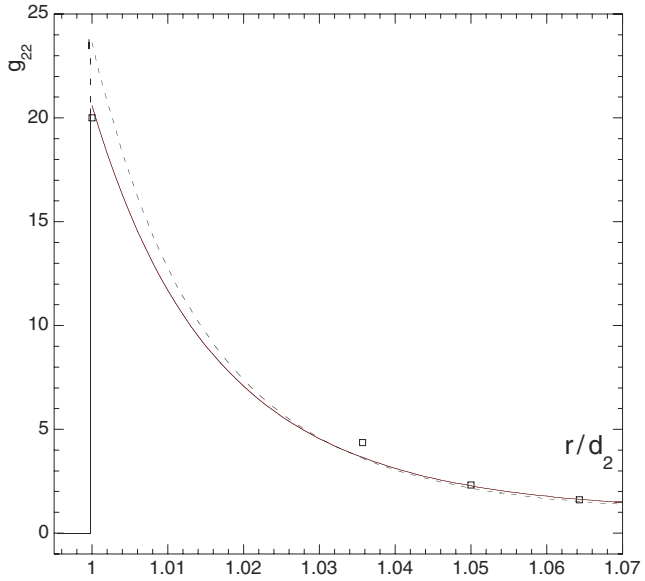

Figure 4. $g_{22}^{\rm eff}$ versus $g_{22}^{\rm mix}$ of figure 3. Full curve: $g_{22}^{\rm mix}$; broken curve: $g_{22}^{\rm eff}$ ($\eta_1^{\rm b} = 0.127$). Symbols: same as in figure 3.

(This figure is in colour only in the electronic version)

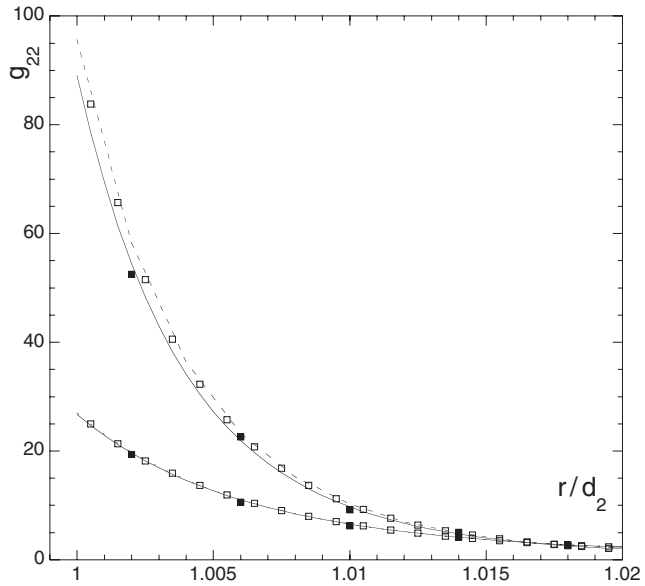

Figure 5. Solute pdfs for $R = 20$, $\eta_2 = 0.097$. Lower set: $\eta_1^{\rm b} = 0.1$, $\eta_1 = 0.089$; upper set: $\eta_1^{\rm b} = 0.14$, $\eta_1 = 0.127$. Full curve: $g_{22}^{\rm mix}$; broken curve: $g_{22}^{\rm eff}$. Symbols: simulation; full squares: $g_{22}^{\rm mix}$; empty squares: $g_{22}^{\rm eff}$.

It should be mentioned that, at larger distances, $g_{22}^{\rm mix}$ might fall below $g_{22}^{\rm eff}$. This suggests that at large η_2 the effect of the PIA can be subtle beyond the contact region.

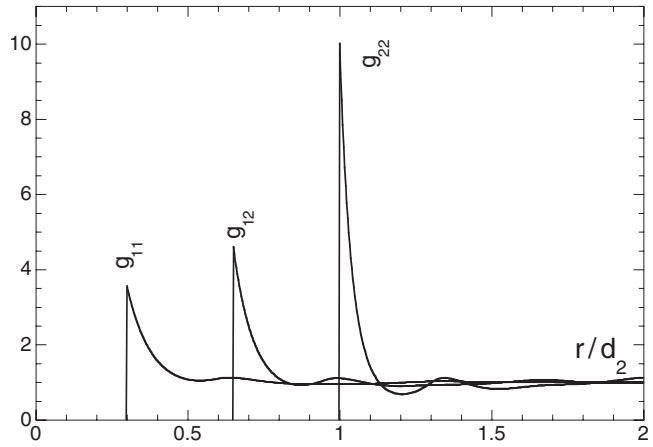

Figure 6. PDFs in a mixture with $R = 3.33$, $\eta_1 = 0.141$, $\eta_2 = 0.348$. Full curves: DFT.

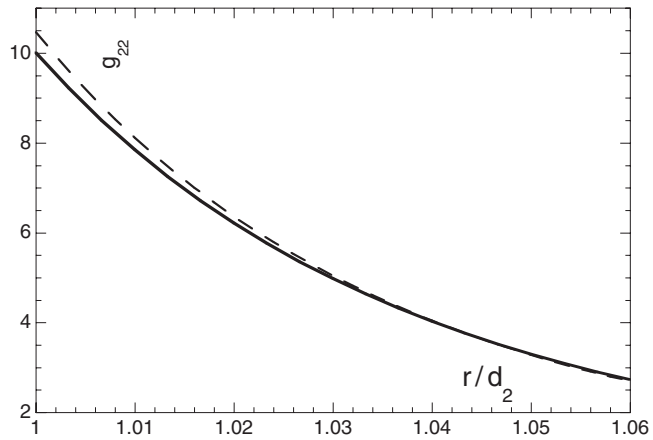

Figure 7. g_{22}^{eff} versus g_{22}^{mix} of figure 6. Full curve: g_{22}^{mix}; broken curve: g_{22}^{eff} ($\eta_1^{\mathrm{b}} = 0.288$).

In conclusion, we may say that at $R = 10$ an overestimation of the 'contact adhesion' in the effective fluid is detectable, but its influence remains moderate, at least in the regime of the reservoir solvent packing fraction explored here ($\eta_1^{\mathrm{b}} \leqslant 0.17$).

A result for $R = 20$ is shown in figure 5. The trend observed for $R = 10$ is observed again but the overestimation of the pdf is barely distinguishable. Note that new simulation data for the effective fluid that we obtained very recently are displayed instead of the previous ones. These were obtained with a lower number of large spheres and a too large histogram width. Figure 5 suggests that $R = 20$ is close to the upper limit at which non-additivity effects might be detected.

Finally, figures 6 and 7 show the result $R = 3.33$ (simulation data of [19] for $d_1/d_2 = 0.3$). At this lower asymmetry the RHNC or DFT work quite well (see [11] for a comparison of the latter with the simulation data of [19]). Unexpectedly, the difference between g_{22}^{mix} and g_{22}^{eff} is similar to that at $R = 10$. For a much less asymmetric case, one would have expected a more obvious manifestation of non-additivity (the RHNC results suggest an even lower effect of the PIA). Whether a larger effect would be obtained at larger η_1^{b} remains to be investigated. This shows that the dependence on the size ratio of the difference between g_{22}^{mix} and g_{22}^{eff} is not simple.

3.3. Discussion

The results shown above suggest that a moderate effect of the PIA is detectable for size ratios $R \leqslant 20$. The simplest explanation of this observation is that the distribution of the solvent $\rho^1(r; R_1, R_2)$ around two spheres nearly in contact should be disturbed by additional spheres. In a triplet, for example, the actual effective force acting on solute 1 due to the presence of the two other solutes (2 and 3) $\vec{F}_1(2, 3)$ would differ from the sum between pairs $\vec{F}_1(2) + \vec{F}_1(3)$ where $\vec{F}_1(i)$ is the effective force acting on solute particle 1 due to solute i. This superposition approximation of the force is obviously equivalent to the PIA. The overestimation might now be due to the neglect of the confinement effect which would increase the solvent density in the channel between the large spheres when a third sphere approaches. This confined solvent contributes to a repulsion when the separation between the surface of the large spheres is less than one solvent diameter [21–23]. These effects should, of course, depend on the solvent–solute correlation length and a third sphere whose minimum distance of approach is larger than this length would barely affect $\rho^1(r; R_1, R_2)$. This can be viewed as a generalization of the geometrical argument invoked in Asakura–Oosawa-like models [24]. The latter is based on the impossibility of the simultaneous overlap of the three exclusion spheres beyond some ratio $R_{\rm lim}$.

Since some understanding of the origin of the overestimation of the effective adhesion might suggest simple ways to correct the PIA, we attempted to detect non-additivity of the mean force directly by simulation, as done for example in [25] for $R = 1$. In our previous work, we reported a difference between the superposition approximation and the actual mean force measured in a diamond configuration of four spheres (see the second line of table 2 in [2]). The force is obtained by extrapolating at contact the ensemble average $\sum_i \langle \cos\theta_i \rangle$, where θ_i is the azimuthal angle between the position r_i of the ith solvent particle and the axis along the direction of the measured force. The accuracy of the result depends on the method of extrapolation. From the extensive checks we performed, we consider now that the difference $\vec{F}_1(2, 3) - [\vec{F}_1(2) + \vec{F}_1(3)]$ is within numerical uncertainty for $R = 10$. Recent attempts to modify the separation between the spheres and the solvent density were also inconclusive. We are presently considering non-planar configurations in order to try to detect this apparently tiny effect (see also the discussion of this point in [4]).

From these considerations, we finally suggested [2] that the phase diagram of the mixture should not differ qualitatively from that in the effective fluid with only pair interactions. The main expected effect is an increase of the separation between the (metastable) fluid–fluid boundary and the fluid–solid one. Some caution is, however, required since simulation data are lacking when both $\eta_1^{\rm b}$ and η_2 are 'large'.

4. Conclusion

As a brief conclusion, we may say that deviations from the PIA were detected in HS mixtures for size ratios as large as $R = 20$, but their effect is estimated as moderate. It was also observed that recent integral equation and DFT theories can capture this effect. This opens up the possibility of a systematic exploration of the phase diagram in order to firmly establish the domain of validity of this approximation. An interpretation in terms of the modification of the solvent distribution about the spheres suggests a rationale for the observed overestimation of the effective adhesion near contact. It also suggests that in non-HS systems possible long range solute–solvent correlations might enhance the role of such many-body effects. Attempts to correct this approximation by accounting for the presence of terms beyond second order might be more relevant in this case.

References

[1] *Discussions of the Workshop on Many-body Interactions and Correlations in Soft Matter (Lyon, 2003)* this issue
[2] Malherbe J G and Amokrane S 2001 *Mol. Phys.* **99** 355
[3] Dijkstra M and van Roij R 2002 *Phys. Rev. Lett.* **89** 208303
[4] Biben T, Bladon P and Frenkel D 1996 *J. Phys.: Condens. Matter* **8** 10799
[5] Dijkstra M, van Roij R and Evans R 1999 *Phys. Rev.* E **59** 5744
[6] Germain P, Regnaut C and Amokrane S 2003 *Phys. Rev.* E **67** 061101
[7] Roth R, Evans R and Louis A A 2001 *Phys. Rev.* E **64** 051202
[8] Rosenfeld Y 1993 *J. Chem. Phys.* **98** 8126
[9] Evans R 1992 *Fundamentals of Inhomogeneous Fluids* ed D Henderson (New York: Dekker) p 85
[10] Roth R, Evans R, Lang A and Kahl G 2002 *J. Phys.: Condens. Matter* **14** 12063
[11] Yu Y and Wu J 2002 *J. Chem. Phys.* **117** 10156
[12] Boublik T 1970 *J. Chem. Phys.* **53** 471
Mansoori G A, Carnahan N F, Starling K E and Leland T W Jr 1971 *J. Chem. Phys.* **54** 1523
[13] Rosenfeld Y 1995 *J. Phys. Chem.* **99** 2857
[14] Archer A J and Evans R 2003 *J. Chem. Phys.* **118** 9726
[15] Amokrane S and Malherbe J D 2001 *J. Phys.: Condens. Matter* **13** 7199
Amokrane S and Malherbe J D 2002 *J. Phys.: Condens. Matter* **14** 3845 (erratum)
[16] Roth R, Evans R and Dietrich S 2000 *Phys. Rev.* E **62** 5360
[17] Clement-Cottuz J, Amokrane S and Regnaut C 2000 *Phys. Rev.* E **61** 1692
[18] Lue L and Woodcock L V 1999 *Mol. Phys.* **96** 1435
[19] Malijewsky A, Barosova M and Smith W R 1996 *Mol. Phys.* **91** 65
[20] Dress C and Krauth W 1995 *J. Phys. A: Math. Gen.* **28** L597
Buhot A and Krauth W 1998 *Phys. Rev. Lett.* **80** 3787
[21] Attard P 1989 *J. Chem. Phys.* **91** 3083
[22] Dickman R, Attard P and Simonian V 1997 *J. Chem. Phys.* **107** 205
[23] Attard P 1991 *J. Chem. Phys.* **95** 4471
[24] Asakura S and Oosawa F 1954 *J. Chem. Phys.* **22** 1255
[25] Tehver R, Maritan A, Koplik J and Banavar R 1999 *Phys. Rev.* E **59** 1339